Research paper

# Changes in spontaneous and odorant-induced single-unit activity of mitral/tufted neurons of the rat olfactory bulb during xylazine-tiletamine-zolazepam anesthesia

V.N. Kiroy [a], P.O. Kosenko [a,*], A.B. Smolikov [a], A.I. Saevskiy [a], E.V. Aslanyan [a], P.D. Shaposhnikov [a], Yu.A. Rebrov [a], F.V. Arsenyev [b]

[a] *Southern Federal University, Rostov-on-Don, Russia*
[b] *Foundation for Advanced Research of Russia, Russia*

## ARTICLE INFO

## ABSTRACT

The nature and severity of mitral/tufted (M/T) cells reactions to odorants presented in anesthesia depend on various factors, and, above all, the nature and concentration of the odor, anesthesia, and the functional state of the olfactory bulb (OB). Compared to wakefulness, under anesthesia, the intensity of OB M/T cells responses to the odorants presented increases. However, the influence of anesthesia dynamics on the intensity of such responses has not been studied. To address this problem in rats, the activity of M/T cells and the local field potentials (LFP) in OB were recorded in the course of xylazine-tiletamine-zolazepam (XTZ) anesthesia. It has been shown that in the course of the anesthesia, the average frequency of background and odorant-induced single-unit activity of M/T cells increases, while the dominant frequency value of LFP in the gamma frequency range (90–170 Hz), on the contrary, decreases. The observed effects are assumed to be associated with changes in the functional state of the OB and systems for processing olfactory information in anesthesia.

## 1. Introduction

LFP and single-unit activity of OB neurons induced by the presentation of odorants is known to significantly depend on whether the recording is conducted in an awake animal or under anesthesia (Rinberg et al., 2006; Cury and Uchida, 2010; Shusterman et al., 2011; Wachowiak, 2011). In the latter case attention is primarily drawn to the nature of anesthesia (Neville and Haberly, 2003; Li et al., 2012; Chery et al., 2014). However, it is also known that anesthesia is a dynamic process that includes several phases, including transitions from wakefulness to anesthesia and back to wakefulness (Yoon et al., 2011; Esteves et al. 2019). We have previously shown (Kosenko et al., 2020) that the use of XTZ anesthesia leads to phase changes in the functional state of the OB, which is most clearly manifested at the gamma frequencies (91–170 Hz) of the OB LFP. Given these circumstances, it can be expected that the nature of OB activity caused by the presentation of odorants depends not only on the presence or absence of anesthesia and its nature, but also on its phase. However, this aspect of the problem has not yet been given due attention.

The purpose of this study was to investigate the nature and severity of the background and odorant-induced single-unit activity of M/T neurons in the OB of rats during XTZ anesthesia. To the best of our knowledge, this is the first study to examine the effect of XTZ anesthesia on the temporal dynamics of the odor-induced bioelectrical activity of neurons and neuronal populations in rat OB.

## 2. Experimental procedures

### 2.1. Materials and methods

The experiments involved 8 adult male Norway rats (*Rattus norvegicus*; weight, 350–450 g), which were housed in individual microisolators (54 cm × 39 cm × 21 cm, sawdust bedding) at constant temperature (23 ± 1 °C) and humidity, and a 12/12 h light/dark cycle. Rats had ad libitum access to food (complete extruded combo feed for laboratory animals, JSC Gatchinskiy compound feed plant) and reverse-osmosis purified water. All experimental and animal care procedures followed Directives 2010/63/EU of the European Parliament and of the

Council of 22 September 2010 on the protection of animals used for scientific purposes and were also approved in advance by The Animal Ethics Committee of Southern Federal University (Rostov on Don, Russia).

### 2.2. Surgery

For simultaneous recording of LFP and single-unit activity of OB neurons, sharpened glass-coated tungsten microelectrodes (ø 50 μm in their thick part) were used. The microelectrodes were assembled into arrays of 8–16 electrodes (differences in the number of electrodes were determined by research protocols) with an interelectrode distance of 500 μm (2–4 lines with 4 electrodes each), which ensured the recording of different M/T neurons activity (Buonviso et al., 1991). Arrays of the microelectrodes were implanted under XTZ anesthesia in the OB of rats to a depth of about 400 μm below dura where M/T cells are predominantly located (Gao et al., 2018). All surgical procedures for the implantation of microelectrode arrays and the postoperative recovery period are described in detail in our previous publication (Kosenko et al., 2020). The recovery period after the implantation surgery was at least one week before the first experiments.

### 2.3. Recording of OB bioelectrical activity and odorant presentation

The recording of LFP and the single-unit activity of OB neurons was carried out in rats under XTZ anesthesia in a rectangular chamber (100 cm × 50 cm) inside a Faraday cage using a 32-channel Plexon Multichannel Acquisition Processor (MAP) data acquisition system (Plexon Corp., Dallas, Texas) with a sampling rate of 10 kHz for each channel. The Plexon data acquisition system consisted of a signal preamplifier, a Plexon amplifier, and a PC with the Plexon-Sort Client software installed. The preamplifier received cell activity recorded by the microelectrodes. From the preamplifier, the recorded signals were fed to the amplifier input SIG (signal input board), where programmable amplification and analog-to-digital conversion of the recorded signals were performed. Next, the signals were sent to the DSP (digital signal processor) module, where the single-unit activity was sorted. Synchronization of single-unit activity and LFP with the moment of olfactory stimulus presentation was carried out using TIM and HLK2 boards placed on a Plexon MAP-32 amplifier. All data was buffered on the server, allowing real-time access to them using the Sort Client software.

The single-unit activity was extracted using the Offline Sorter software package (Plexon Inc.). Action potentials, or spikes of neurons, were identified using the principal component method (Lewicki, 1998) based on their shapes and amplitudes (Jackson and Fetz, 2007) recorded during first 10 min since the anesthesia onset. When extracting spikes from a raw signal, it is assumed that each neuron generates spikes of a unique shape and constant amplitude, so the spikes of the same shape and amplitude were assigned to the same neuron. Automatic spike detection was evaluated and corrected using manual sorting: distant and dense clusters of points were considered belonging to different neurons (Wood and Black, 2008). Artifacts or spikes generated by unsorted neurons located far from the recording electrode and differing from the main spikes in the shape and amplitude were excluded from the analysis.

The presentation of the gas-air mixture containing the tobacco odorant was carried out using the originally designed odorizer; its block diagram is shown in Fig. 1. Air from the environment, heated to room temperature, was supplied by a compressor to plastic bags located in two hermetically sealed 15-liter cylinders. The filling bags displaced the gas-air mixture containing either clean air passing through filters or the tobacco odorant. The tobacco odorant was kept in a separate cylinder and was prepared as follows: 10 g of tobacco were placed in a single layer gauze tampon at the bottom of the cylinder filled with clean air and kept for 12 h after the tampon was immersed.

The valve system located further on programmatically controlled the moments and duration of the presentations of the gas-air mixture containing the tobacco odorant or clean air. The duration of a single sample presentation was 5 s, the flow rate was 2 liters per minute. During 55 s of interstimulus interval clean air was supplied with the same intensity.

According to the protocol, a total of 90 stimuli were presented to a single animal during an experiment. Thus, considering the number and duration of stimuli presented, as well as the duration of each interstimulus interval, the total duration of an experiment was up to 90 min. The stimuli were combined into cycles of 10 presentations falling within the 10 min time windows.

Analysis methods.

The single-unit activity of OB M/T cells was analyzed using Neuro-Explorer4 software (Nex Technologies). The analysis included the creation of peristimulus raster plots and histograms, the calculation of the average frequency of M/T neurons single-unit activity at 5-s epochs recorded immediately before and during the presentation of a gas-air mixture containing the tobacco odorant.

The analysis of the LFP recorded from the same electrodes included the calculation of the dominant frequency of the OB LFP in the gamma range, which was performed as follows:

(a) the data series was downsampled to 1 kHz and divided into 1-
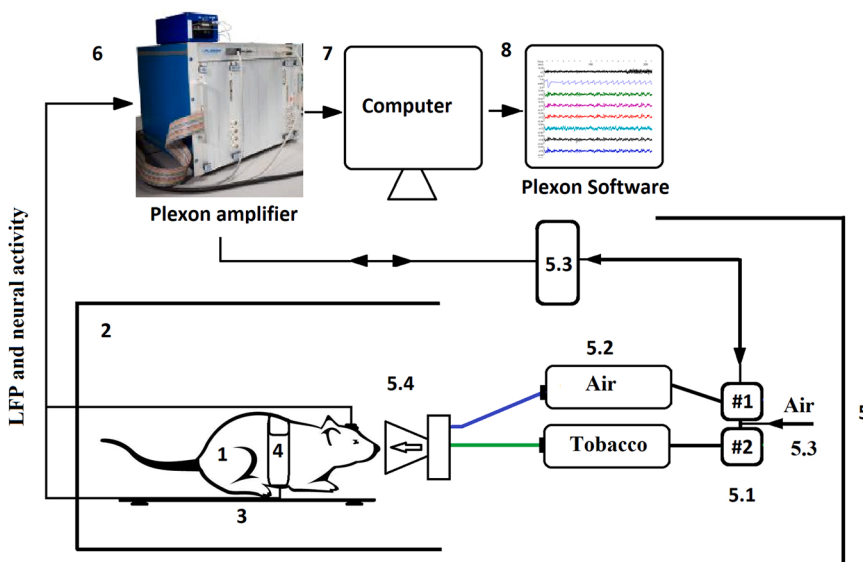


**Fig. 1.** Schematic of the experimental system for the registration of LFP and single-unit activity of rat OB neurons during presentation of either clean air or the gas-air mixture containing the tobacco odorant, Designations: 1 - an anesthetized rat with an implanted microelectrode array that ensures the recording of LFP and single-unit activity from the OB dorsal surface; 2 - experimental chamber (box); 3 - system for automatically maintaining the temperature of the animal's body; 4 - breathing control system; 5 – odorant presentation system; 5.1 - valves; 5.2-15-liter cylinders containing gas-air mixtures; 5.3 - air injected by the compressor; 5.4 - mask for supplying the gas-air mixture; 5.5 - valve control board; 6–32-channel system Plexon Multichannel Acquisition Processor (Plexon Corp., Dallas, Texas, USA); 7 - PC; 8 - Plexon software.

minute fragments,

(b) using the Welch method (Welch, 1967) and the Hanning window, the spectral power of the gamma rhythm was calculated in a sliding time window of 1024 points with a 50% window overlap for each 1-minute fragment,

(c) from the periodogram obtained for each 1-minute fragment, the dominant frequency was extracted as one corresponding to the largest power spectral density value,

(e) a time series of the dominant gamma frequency was formed, with each point corresponding to consecutive 1-minute fragments.

As a result, for each OB LFP recording, a series of about 90 values of the dominant gamma frequencies was formed, which could also be split into cycles of 10 presentations.

Statistical analysis of the data obtained was performed using ANOVA/MANOVA (repeated measures method followed by planned contrasts and 1-factor analysis (breakdown & one-way ANOVA)), implemented in the Statistica-10 application package. The grouping factors were: "state" (factor levels: "background" (F), "impact" (C)); "cycle" (factor levels: 1–10)). Individual neurons were considered dependent variables (R1). Two levels of significance were used: at $p < 0.05$, the differences were considered significant, at $0.05 < p < 0.08$ they were substantial (the presence of a trend was stated). Differences (in %) were normalized relative to the first indicator in the compared pair according to the formula: F–P (%) = (P – F) / F × 100%. Comparison between the frequencies in the background and the odorant-induced single-unit activity of M/T neurons was carried out using the T-test: at $p < 0.05$, the differences were considered significant. In addition, the Pearson correlation coefficients (CC) between the features of single-unit activity and LFP were calculated.

## 3. Results

### 3.1. M/T neurons activity

Histological control of the animals' samples was performed at the end of the study, and it indicated that the LFP and the single-unit activity of OB neurons were indeed recorded at depths of 400–450 μm. The distinguishing feature of M/T cells is the generation of high-amplitude spikes (up to 400 μV), which is 3–10 times higher than the amplitude of spikes generated by neurons of other types. This often serves as a criterion for sorting recorded neurons. It is also known that, at rest, in anesthetized animals, the average frequency of M/T neurons discharges does not exceed 20 Hz (Chaput et al., 1992).

The identification of M/T neurons was carried out based on the analysis of the single-unit activity recorded during the first 10 min of XTZ anesthesia. A total of 97 neurons were identified in this study. In 58 of them (60%), a reaction to the presentation of the odorant in the form of inhibition or excitation was recorded (T-test; $p < 0.05$, Fig. 2A, B, D).

Based on the analysis, 2 groups of neurons were identified with an average discharge frequency of less than and more than 20 spike/sec. The activity of 36 neurons (out of 58 responding ones) with an average discharge frequency of less than 20 spike/sec met the criteria listed in the first paragraph of the current section, which allowed us to consider these neurons as M/T cells. The average frequency of the background activity of these neurons was $11 \pm 5.79$ spike/sec. In response to the presentation of air samples containing the tobacco odorant, statistically significant changes in the frequency of these neurons' activity were observed, indicating the development of either excitatory or inhibitory reaction (T-test; $p < 0.05$, Fig. 2D).

We further divided those 36 identified M/T-neurons into groups by their response type to the presentation of the olfactory stimulus used. A statistically significant increase in the frequency of discharges (on average, up to $127.3 \pm 9.4\%$) upon presentation of air samples containing the tobacco odorant was observed in 17 (47%) of the M/T cells considered ($F_{9183} = 35.56$; $p < 0.001$, Fig. 2C). In 19 other neurons (53%), the frequency of discharges decreased significantly (on average, to $85.7 \pm 4.3\%$; $F_{9.174} = 390.76$; $p < 0.001$, Fig. 2 C). As follows from the example shown in Fig. 2A, the average frequency of M/T neurons discharges that react with excitation on presentation of air samples containing the tobacco odorant increased up to more than 4 times.

Of the total number (n = 36) of identified M/T neurons, the activity of 20 neurons was recorded throughout the observation time, that is,
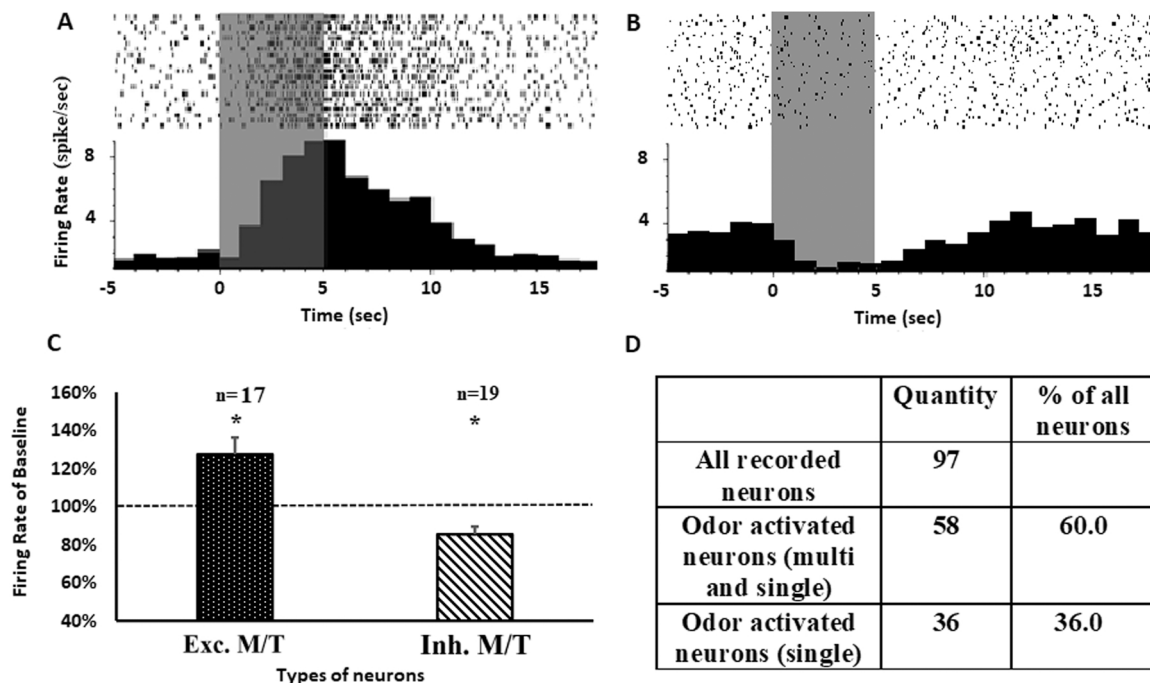


**Fig. 2.** Odorant-induced M/T neuronal activity. Peristimulus raster plots (top, black serifs are spikes) and histograms (bottom) of the spiking activity of neurons that react with excitation (A) and inhibition (B) to the presentation of the tobacco odorant (bin=1 s). 0 – onset of the tobacco odorant sample presentation. The period of odorant presentation is marked with a gray rectangle. (C) - statistical characteristics of the responses of excitatory (Exc.) and inhibitory (Inh.) M/T neurons to the presentation of tobacco odorant. (D) - the number of registered neurons.

90 min from the start of the surgical phase of anesthesia. 9 of them were identified as inhibitory (they reacted to the presentation of the odorant with a decrease in the frequency of discharges), 11 were excitatory (they responded with an increase in the frequency of discharges).

Analysis of activity dynamics in the M/T excitatory neurons revealed

that the background frequency of their discharges ($8.08 \pm 5.3$ spikes/s) practically did not change upon presentation of pure air and remained unchanged approximately within 30 min from the anesthesia onset. Subsequently, an increase in the background frequency of the discharges of these neurons was observed until the end of the recording (90 min
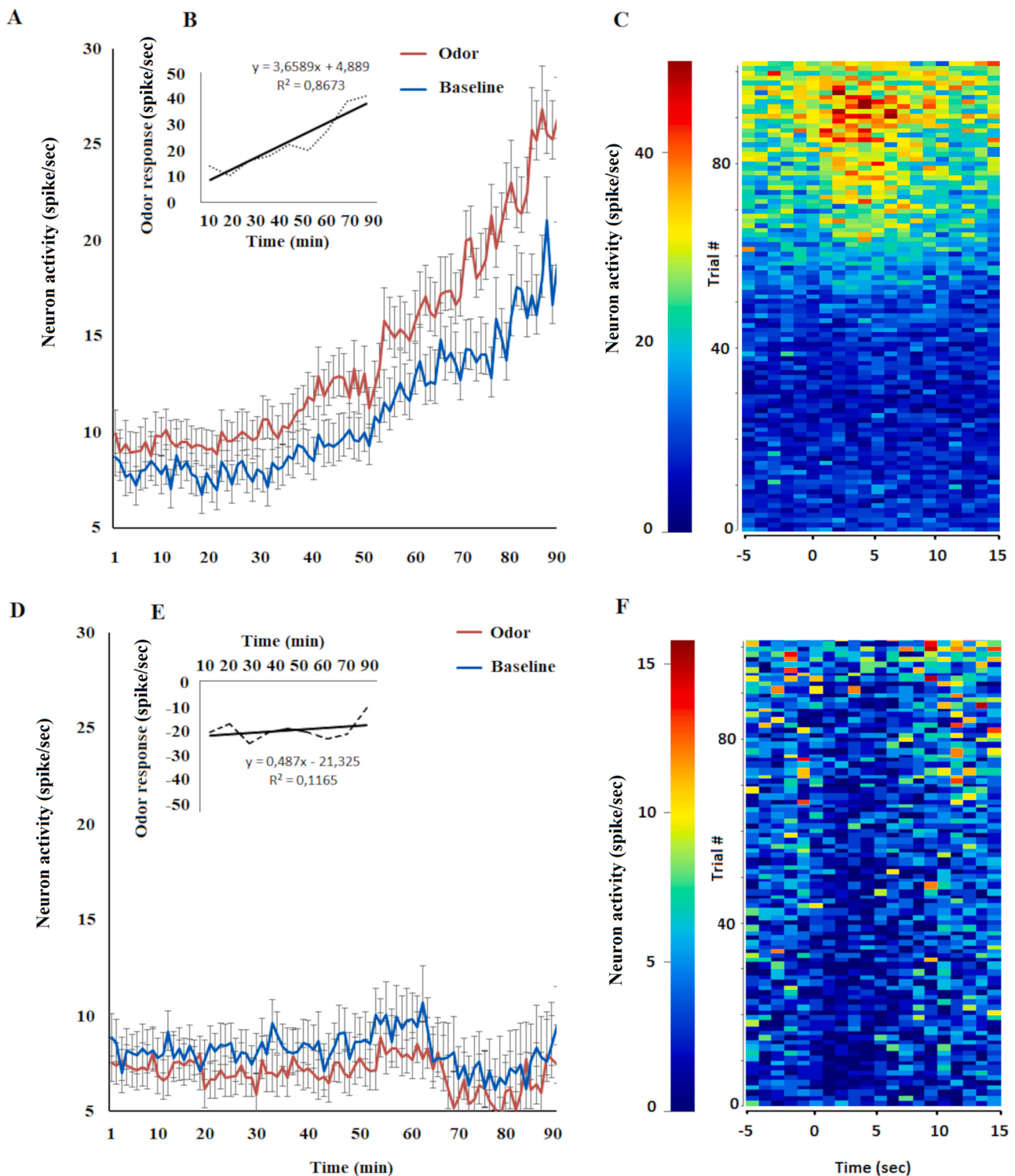


**Fig. 3.** Change in the average frequency of OB M/T neurons discharges, reacting with excitation and inhibition to the presentation of air samples containing the tobacco odorant, (A) - mean frequency values of the background (blue line) and odorant-induced (red line) single-unit activity of excitatory M/T neurons vs. time. (B) - difference in the responses of excitatory neurons between the presentation of the tobacco odorant and air vs. time. (C) - an example of a peristimulus histogram of an excitatory M/T neuron. (D) - mean frequency values of the background (blue line) and odorant-induced (red line) single-unit activity of inhibitory M/T neurons vs. time. (E) - difference in the responses of inhibitory neurons between the presentation of the tobacco odorant and air vs. time. (F) - an example of peristimulus histogram of an inhibitory M/T neuron.

from the anesthesia onset) (Fig. 3 A, B, C).

The dynamics of the discharge frequency of these neurons upon presentation of air samples containing the tobacco odorant was generally identical (Fig. 3A). The difference consisted only in a more significant increase in the frequency of M/T cells discharges in response to the presentation of air samples containing the tobacco odorant after 30 presentations (30 min of anesthesia) (Fig. 3A). As one can see in Fig. 3B, these changes in discharge frequency were generally highly correlated (CC=0.9), even though, as anesthesia developed, there was a trend towards an increase in the difference between the background and odorant-induced firing rate of M/T neurons (Fig. 3A).

There were practically no pronounced changes in the discharge frequency of inhibitory M/T cells both during presentation of clean air and samples containing the tobacco odorant throughout the experiment (Fig. 3F).

The results of a comparative analysis of the average M/T neurons firing rate calculated for 10-minute cycles are presented in Table 1. As the table shows, the difference in the frequency of the single-unit activity recorded immediately before and during presentation of the odorant was statistically significant for both inhibitory and excitatory M/T neurons. However, while, for the former, it practically did not change during the experiment, with changes not exceeding 20%, for the latter, it progressively increased, approaching changes by 40%.

At the same time, while the differences in the frequency of inhibitory M/T neurons discharges at sequentially recorded 10-minute intervals (compared to the first 10-minute cycle) were almost random (Table 2) and statistically insignificant ($F_{Dn}$ (9; 89) = 0.507 p = 0.866), for excitatory neurons, this value increased progressively, reaching 500% at the end of the recording ($F_{In}$ (9; 89) = 31.576 p = 0.000, Fig. 3F). Statistically significant differences were found at an interval of about 50 min from the XTZ anesthesia onset and reached their maximum at the end of the recording.

Examples of raw OB LFP recording, pneumograms and cardiograms are shown in Fig. 4A. The development of XTZ anesthesia was accompanied by a change in the spectral characteristics of the OB LFP. In all animals, they consisted in a decrease of the dominant gamma frequency (Fig. 4B, C), which reached a minimum at about 80 min from the anesthesia onset (Fig. 4C).

To investigate general trends in dominant gamma frequency and odor-induced excitatory M/T activity dynamics and relationship between them, we averaged the corresponding data among animals (Fig. 4C) and then calculated the Pearson correlation coefficient. Since it is of practical use to odor recognition, we calculated response efficiency (difference between the background and odorant-induced single-unit firing rate) rather than just odor-induced firing rate. The analysis showed that, in the group of excitatory M/T neurons, there are antiphase relationships between the response efficiency and the dominant gamma frequency (CC=−0.899, Fig. 4C), while, in inhibitory neurons, no correlation was found between these indicators (CC = −0.073).

## 4. Discussion

It is well known that M/T neurons are the output elements of OB (Imamura et al., 2020). Studies have shown that the encoding of information in the OB occurs through a change in the frequency of spiking activity and the formation of specific activity patterns in these neurons, followed by decoding in higher structures, in particular, pyramidal neurons of the piriform cortex (Yokoi et al., 1995; Cang and Isaacson, 2003; Bathellier et al., 2008; Uchida et al., 2014). At the same time, the presentation of odorants can cause both an increase (excitation) in the single-unit activity of M/T neurons and a decrease (inhibition) (Yokoi et al., 1995; Cang and Isaacson, 2003; Rinberg et al., 2006; Bathellier et al., 2008; Shmuel et al., 2019), which is consistent with our results. Under anesthesia (compared to wakefulness), responses to odorants are recorded in a significant number of M/T neurons (Nagayama et al., 2004; Davison and Katz, 2007; Bathellier et al., 2008; Fantana et al., 2008; Khan et al., 2008; Tan et al., 2010), which is also consistent with our results, according to which about 37% of the registered cells reacted by excitation or inhibition to the presentation of air samples containing the tobacco odorant. Their direct participation in the mechanisms of processing the information about the odorants contained in these samples may be indicated by the fact that, as was shown earlier, neurons responding with a change in the frequency of discharges, as a rule, respond only to a small number of odorants with similar properties (Davison and Katz, 2007; Fantana et al., 2008; Tan et al., 2010).

It is also known that, in awake rodents, the frequency of M/T cells spontaneous discharges is higher than in anesthetized animals, and on averages is 10–25 spike/s (Uchida et al., 2014). The average discharge frequency of excitatory M/T neurons in response to samples containing the tobacco odorant at the beginning of the anesthesia was 8.08 ± 5.3 spike/s and at the end of the anesthesia - 17.67 ± 7.58 spike/s.

In wakefulness, the nature and severity of M/T neurons' reaction to the odorant presentation depend on the number of factors. "Silent" M/T neurons with no or weak background firing rate were shown to demonstrate a high firing rate in response to odorants, while M/T neurons with a higher background firing rate have a weak response (Kollo et al., 2014). Moreover, the background and odorant-induced activity of M/T neurons depends on the state of the animal and the nature of the task being executed (Kay and Laurent, 1999).

As noted above, anesthesia has a significant effect on the activity of OB neurons. It has been shown that, compared to wakefulness, under anesthesia, the intensity of OB M/T cells responses to the presented odorants increases, and during recovery from anesthesia, the sensitivity of M/T neurons, on the contrary, decreases (Rinberg et al., 2004, Li et al., 2011).

In our study, it was shown that (1) changes in the activity of M/T neurons under conditions of XTZ anesthesia are of a phase nature, both in the presence and absence of olfactory stimulation, and (2) are observed only in M/T neurons that respond by an increase in the

**Table 1**
Results of MANOVA of the average frequency values of M/T neurons discharges induced by presentation of the odorant, compared to the preceding background (F-V) (only m.e., df eff. are provided; err. = 1; 18).

| Neuron type | Cycle | F | p | % | Neuron type | Cycle | F | P | % |
|---|---|---|---|---|---|---|---|---|---|
| **Inhibitory neurons** | 1 | 17,47 | 0,0000 | -19,54 | **Excitatory neurons** | 1 | 5,80 | 0,0170 | 13,89 |
| | 2 | 10,32 | 0,0016 | -16,32 | | 2 | 3,19 | 0,0759 | 10,41 |
| | 3 | 20,43 | 0,0000 | -24,00 | | 3 | 7,70 | 0,0061 | 16,17 |
| | 4 | 12,14 | 0,0006 | -19,68 | | 4 | 10,63 | 0,0013 | 18,02 |
| | 5 | 9,15 | 0,0029 | -18,23 | | 5 | 21,03 | 0,0000 | 22,34 |
| | 6 | 13,64 | 0,0003 | -19,62 | | 6 | 26,24 | 0,0000 | 20,06 |
| | 7 | 23,03 | 0,0000 | -22,07 | | 7 | 66,17 | 0,0000 | 27,68 |
| | 8 | 19,07 | 0,0000 | -20,32 | | 8 | 153,78 | 0,0000 | 39,00 |
| | 9 | 7,13 | 0,0083 | -10,22 | | 9 | 237,54 | 0,0000 | 41,07 |
| | All | 30,90 | 0,0000 | -18,08 | | All | 16,86 | 0,0001 | 26,32 |

Designations: F - Fisher test, p - significance level, % - difference between background and odorant presentation normalized by background, red font - significant, blue font - trend (for all 9 degrees of freedom; 193).

**Table 2**
Results of MANOVA of the difference in the average frequency values of M/T neurons discharges during the odorant presentation and in the background during XTZ anesthesia (all designations are inherited from Table 1).

| Neuron type | Cycle | F | p | % | Neuron type | Cycle | F | P | % |
|---|---|---|---|---|---|---|---|---|---|
| **Inhibitory neurons** | 1–2 | 0,494623 | 0,483708 | -23,13 | **Excitatory neurons** | 1–2 | 0,281770 | 0,596896 | -25,88 |
| | 1–3 | 0,061466 | 0,804764 | 8,15 | | 1–3 | 0,097075 | 0,756114 | 15,19 |
| | 1–4 | 0,256003 | 0,614131 | -16,64 | | 1–4 | 0,331005 | 0,566553 | 28,05 |
| | 1–5 | 0,705442 | 0,403212 | -27,62 | | 1–5 | 3,433332 | 0,067283 | 90,35 |
| | 1–6 | 0,125441 | 0,724044 | -11,65 | | 1–6 | 5,334080 | 0,023281 | 112,62 |
| | 1–7 | 0,202780 | 0,653581 | 14,81 | | 1–7 | 23,74609 | 0,000005 | 237,62 |
| | 1–8 | 0,018663 | 0,891647 | 4,49 | | 1–8 | 72,32930 | 0,000000 | 414,71 |
| | 1–9 | 1,205492 | 0,275188 | -36,11 | | 1–9 | 122,5028 | 0,000000 | 539,71 |

Relationship between the single-unit activity of M/T neurons and the dominant gamma frequency during XTZ anesthesia.
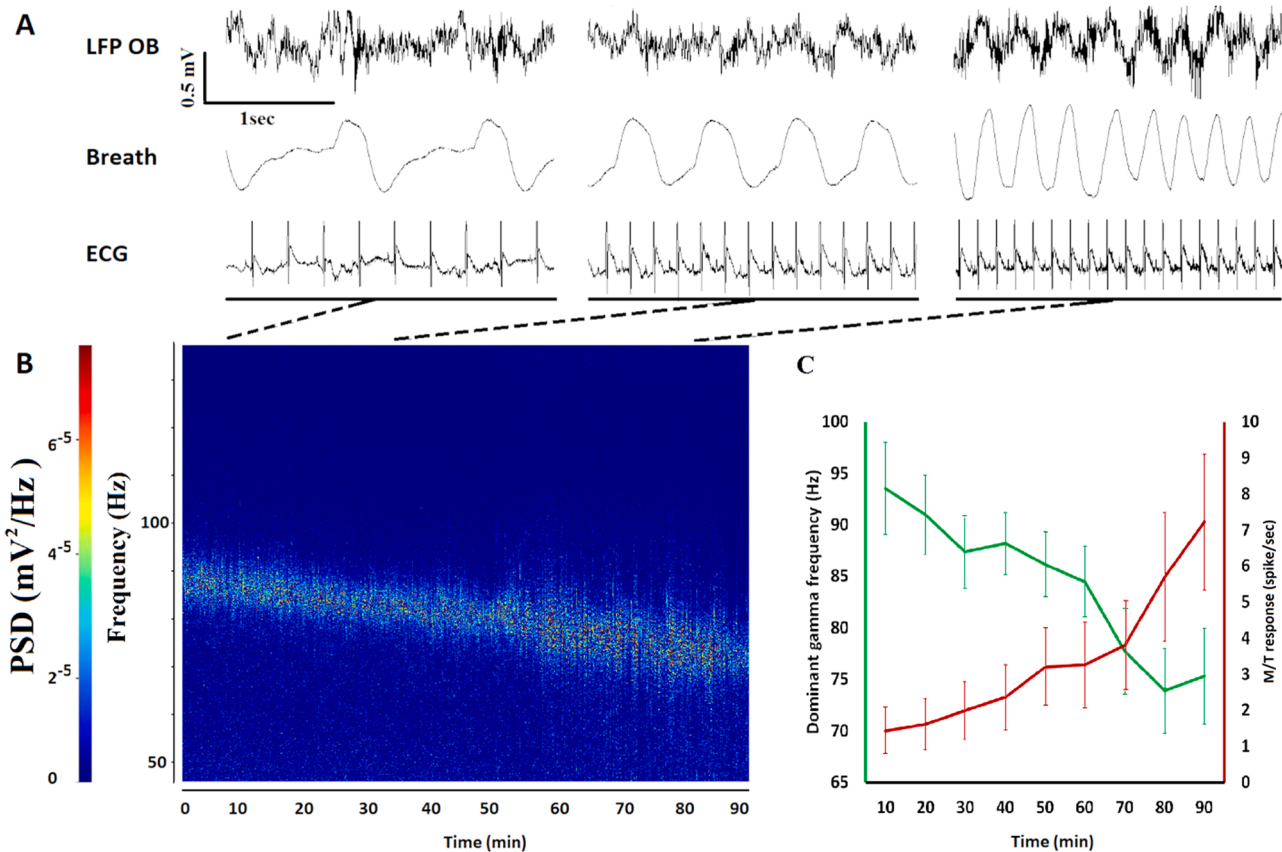


**Fig. 4.** Changes in the OB LFP at the gamma frequencies and the activity of M/T cells during the XTZ anesthesia, (A) - an example of raw OB LFP recordings, pneumogram, and electrocardiogram. (B) – an example of the OB LFP spectrogram in the gamma range. (C) - average values of the dominant gamma frequency (green line) and change in excitatory M/T neurons' firing rates with the presentation of tobacco odorant (difference between odor-induced and baseline firing rates) (red line).

discharge frequency on presentation of air samples containing the tobacco odorant. At the beginning of anesthesia (within 30–40 min), in this group of M/T neurons, an increase in the frequency of discharges was observed both in response to the presentation of air samples containing the tobacco odorant and clean air. This leads to the absence of statistically significant differences and may indicate an increase in perception thresholds related to an increase in the level of M/T neurons activation as a result of a decrease in the level of descending (inhibitory) control. After 75 min of anesthesia, in the initial stages of recovery, due to a more pronounced increase in the frequency of tobacco odorant-induced M/T neurons discharges, the differences become statistically significant, indicating a decrease in perception thresholds.

Changes in both spontaneous and odorant-induced single-unit activity of M/T neurons were clearly correlated with changes in the dominant gamma frequency of OB LFP. Interestingly, for excitatory M/T neurons, this correlation was significantly negative.

The relationship between single-unit activity of neurons and LFP was manifested in several papers. It has been shown that under urethane anesthesia, the activity of M/T neurons in rodents is phase-dependent on the gamma frequency band of OB LFP (Kashiwadani et al., 1999). This band is sometimes considered as the mechanism for time windows formation, during which single-unit activity of neurons is synchronized and processing of olfactory information is performed (Laurent et al., 2001). When the duration of the window increases (which occurs when the frequency is reduced), it becomes possible to "squeeze" in a much larger number of M/T cells discharges, which can provide an increase in the frequency of discharges and allows synchronizing them. It is believed that the correlation of M/T neuron single-unit activity and LFP at the gamma frequencies can facilitate "connection through coherence" (Fries, 2005, Cenier et al., 2009) and information propagation to the cortex

(Litaudon et al., 2008).

In existing source analysis studies (Neville and Haberly, 2003), it was shown that gamma and beta oscillations of the OB LFP are generated by synaptic currents generated predominantly by granule cells. In the frequency range of 60–90 Hz, referred to as the gamma-1 rhythm, 2 subranges are sometimes distinguished (Kay, 2015). The first includes oscillations with a frequency of about 90 Hz (gamma-1.1), which occur at the end of inhalation or the beginning of exhalation, followed by slower oscillations with a frequency of about 70 Hz, which are attributed to the second subrange – gamma-1.2. It is assumed that faster gamma-1.1 oscillations are associated with the activity of tufted cells that receive direct inputs from olfactory neurons and have a lower sensitivity threshold than mitral cells (Gire et al., 2012; Geramita et al., 2016). Tufted cells discharge at the peak of inhalation with little deviations (Fukunaga et al., 2012). The slower gamma-1.2 oscillations are believed to arise from the activity of mitral cells (Manabe and Mori, 2013), which also receive direct input from olfactory neurons. Both mitral and tufted cells process afferent olfactory sensory information simultaneously and are two separate channels for the output of information from the OB (Geramita et al., 2016; Vaaga and Westbrook, 2016). It is also known that a weak direct input from receptor neurons to M/T neurons is enhanced by multistage excitation, each element of which can modulate the responses of M/T neurons and their subsequent transmission to the higher brain regions (Boyd et al., 2012).

All this suggests that the different dynamics of the background and the odorant-induced activity of inhibitory and excitatory M/T neurons can be determined both by their assignment to different subtypes and by the multidirectional influence of the entire complex of OB neural networks during XTZ anesthesia. Our results show that the level of background and odorant-induced LFP and single-unit activity of M/T neurons changes during XTZ of anesthesia; the relationship between neuronal activity and the dominant gamma frequency was demonstrated, indicating functional rearrangements occurring both at the cellular and system (multicellular) levels of the OB. The results of this study can be useful in the development of bioelectronic noses (biohybrid olfactory systems) based on the single-unit activity and LFP of rat OB.

## CRediT authorship contribution statement

V.N. Kiroy designed the study and wrote the manuscript, performed the final analysis, P.O. Kosenko designed the study and wrote the manuscript, performed surgeries, and conducted the experiments, performed the final analysis, A.B. Smolikov performed surgeries and conducted the experiments, E.V. Aslanyan performed the final analysis, A.I. Saevskiy conducted the experiments, wrote the manuscript, performed the final analysis, Yu.A. Rebrov conducted the experiments, F.V. Arseniev designed the study and wrote the manuscript, P.D. Shaposhnikov conducted the experiments, All authors have approved the final manuscript.

## Conflict of interest

There are no conflicts of interest to disclose.

## Acknowledgments

## References

Bathellier, B., Buhl, D.L., Accolla, R., Carleton, A., 2008. Dynamic ensemble odor coding in the mammalian olfactory bulb: sensory information at different timescales. Neuron 57 (4), 586–598. https://doi.org/10.1016/j.neuron.2008.02.011.

Boyd, A.M., Sturgill, J.F., Poo, C., Isaacson, J.S., 2012. Cortical feedback control of olfactory bulb circuits. Neuron 76 (6), 1161–1174.

Buonviso, N., Chaput, M.A., Scott, J.W., 1991. Mitral cell-to-glomerulus connectivity: an HRP study of the orientation of mitral cell apical dendrites. J. Comp. Neurol. 307 (1), 57–64. https://doi.org/10.1002/cne.903070106.

Cang, J., Isaacson, J.S., 2003. In vivo whole-cell recording of odor-evoked synaptic transmission in the rat olfactory bulb. J. Neurosci. 23 (10), 4108–4116. https://doi.org/10.1523/JNEUROSCI.23-10-04108.2003. PMID: 12764098; PMCID: PMC6741073.

Cenier, T., David, F., Litaudon, P., Garcia, S., Amat, C., Buonviso, N., 2009. Respiration-gated formation of gamma and beta neural assemblies in the mammalian olfactory bulb. Eur. J. Neurosci. 29 (5), 921–930. https://doi.org/10.1111/j.1460-9568.2009.06651.x.

Chaput, M.A., Buonviso, N., Berthommier, F., 1992. Temporal patterns in spontaneous and odour-evoked mitral cell discharges recorded in anaesthetized freely breathing animals. Eur. J. Neurosci. 4 (9), 813–822. https://doi.org/10.1111/j.1460-9568.1992.tb00191.x.

Chery, R., Gurden, H., Martin, C., 2014. Anesthetic regimes modulate the temporal dynamics of local field potential in the mouse olfactory bulb. J. Neurophysiol. 111 (5), 908–917. https://doi.org/10.1152/jn.00261.2013.

Cury, K.M., Uchida, N., 2010. Robust odor coding via inhalation-coupled transient activity in the mammalian olfactory bulb. Neuron 68 (3), 570–585. https://doi.org/10.1016/j.neuron.2010.09.040.

Davison, I.G., Katz, L.C., 2007. Sparse and selective odor coding by mitral/tufted neurons in the main olfactory bulb. J. Neurosci. 27 (8), 2091–2101. https://doi.org/10.1523/JNEUROSCI.3779-06.2007. PMID: 17314304; PMCID: PMC6673545.

Esteves, M., Almeida, A.M., Silva, J., Silva Moreira, P., Carvalho, E., Pêgo, J.M., Almeida, A., Sotiropoulos, I., Sousa, N., Leite-Almeida, H., 2019. MORPhA Scale: Behavioral and electroencephalographic validation of a rodent anesthesia scale. J. Neurosci. Methods 324, 108304. https://doi.org/10.1016/j.jneumeth.2019.05.013.

Fantana, A.L., Soucy, E.R., Meister, M., 2008. Rat olfactory bulb mitral cells receive sparse glomerular inputs. Neuron 59 (5), 802–814. https://doi.org/10.1016/j.neuron.2008.07.039.

Fries, P., 2005. A mechanism for cognitive dynamics: neuronal communication through neuronal coherence. Trends Cogn. Sci. 9 (10), 474–480. https://doi.org/10.1016/j.tics.2005.08.011.

Fukunaga, I., Berning, M., Kollo, M., Schmaltz, A., Schaefer, A.T., 2012. Two distinct channels of olfactory bulb output. Neuron 75 (2), 320–329. https://doi.org/10.1016/j.neuron.2012.05.017.

Gao, K., Li, S., Zhuang, L., Qin, Z., Zhang, B., Huang, L., Wang, P., 2018. In vivo bioelectronic nose using transgenic mice for specific odor detection. Biosens. Bioelectron. 102, 150–156. https://doi.org/10.1016/j.bios.2017.08.055.

Geramita, M.A., Burton, S.D., Urban, N.N., 2016. Distinct lateral inhibitory circuits drive parallel processing of sensory information in the mammalian olfactory bulb. Elife 5.

Gire, D.H., Franks, K.M., Zak, J.D., Tanaka, K.F., Whitesell, J.D., Mulligan, A.A., Hen, R., Schoppa, N.E., 2012. Mitral cells in the olfactory bulb are mainly excited through a multistep signaling path. J. Neurosci. 32 (9), 2964–2975. https://doi.org/10.1523/JNEUROSCI.5580-11.2012. PMID: 22378870; PMCID: PMC3467005.

Imamura, F., Ito, A., LaFever, B.J., 2020. Subpopulations of projection neurons in the olfactory bulb. Front Neural Circuits 28 (14), 561822. https://doi.org/10.3389/fncir.2020.561822. PMID: 32982699; PMCID: PMC7485133.

Jackson, A., Fetz, E.E., 2007. Compact movable microwire array for long-term chronic unit recording in cerebral cortex of primates. J. Neurophysiol. 98 (5), 3109–3118.

Kashiwadani, H., Sasaki, Y.F., Uchida, N., Mori, K., 1999. Synchronized oscillatory discharges of mitral/tufted cells with different molecular receptive ranges in the rabbit olfactory bulb. J. Neurophysiol. 82 (4), 1786–1792. https://doi.org/10.1152/jn.1999.82.4.1786.

Kay, L.M., Laurent, G., 1999. Odor- and context-dependent modulation of mitral cell activity in behaving rats. Nat. Neurosci. 2 (11), 1003–1009. https://doi.org/10.1038/14801.

Kay, L.M., 2015. Olfactory system oscillations across phyla. Curr. Opin. Neurobiol. 31, 141–147. https://doi.org/10.1016/j.conb.2014.10.004.

Khan, A.G., Thattai, M., Bhalla, U.S., 2008. Odor representations in the rat olfactory bulb change smoothly with morphing stimuli. Neuron 57 (4), 571–585. https://doi.org/10.1016/j.neuron.2008.01.008. PMID: 18304486; PMCID: PMC2258318.

Kollo, M., Schmaltz, A., Abdelhamid, M., Fukunaga, I., Schaefer, A.T., 2014. 'Silent' mitral cells dominate odor responses in the olfactory bulb of awake mice. Nat. Neurosci. 17 (10), 1313–1315. https://doi.org/10.1038/nn.3768.

Kosenko, P.O., Smolikov, A.B., Voynov, V.B., Shaposhnikov, P.D., Saevskiy, A.I., Kiroy, V.N., 2020. Effect of Xylazine-Tiletamine-Zolazepam on the Local Field Potential of the Rat Olfactory Bulb. Comp. Med 70 (6), 492–498. https://doi.org/10.30802/AALAS-CM-20-990015. Epub 2020 Nov 9. PMID: 33168131; PMCID: PMC7754196.

Laurent, G., Stopfer, M., Friedrich, R.W., Rabinovich, M.I., Volkovskii, A., Abarbanel, H. D., 2001. Odor encoding as an active, dynamical process: experiments, computation, and theory. Annu Rev. Neurosci. 24, 263–297. https://doi.org/10.1146/annurev.neuro.24.1.263.

Lewicki, M.S., 1998. A review of methods for spike sorting: the detection and classification of neural action potentials. Network 9 (4), R53–R78 (Nov).

Li, A., Gong, L., Xu, F., 2011. Brain-state-independent neural representation of peripheral stimulation in rat olfactory bulb. Proc. Natl. Acad. Sci. USA 108 (12), 5087–5092.

Li, A., Zhang, L., Liu, M., Gong, L., Liu, Q., Xu, F., 2012. Effects of different anesthetics on oscillations in the rat olfactory bulb. J. Am. Assoc. Lab Anim. Sci. 51 (4), 458–463. PMID: 23043811; PMCID: PMC3400694.

Litaudon, P., Garcia, S., Buonviso, N., 2008. Strong coupling between pyramidal cell activity and network oscillations in the olfactory cortex. Neuroscience 156 (3), 781–787. https://doi.org/10.1016/j.neuroscience.2008.07.077.

Manabe, H., Mori, K., 2013. Sniff rhythm-paced fast and slow gamma-oscillations in the olfactory bulb: relation to tufted and mitral cells and behavioral states (Oct). J. Neurophysiol. 110 (7), 1593–1599. https://doi.org/10.1152/jn.00379.2013.

Nagayama, S., Takahashi, Y.K., Yoshihara, Y., Mori, K., 2004. Mitral and tufted cells differ in the decoding manner of odor maps in the rat olfactory bulb. J. Neurophysiol. 91 (6), 2532–2540. https://doi.org/10.1152/jn.01266.2003.

Neville, K.R., Haberly, L.B., 2003. Beta and gamma oscillations in the olfactory system of the urethane-anesthetized rat. J. Neurophysiol. 90 (6), 3921–3930. https://doi.org/10.1152/jn.00475.2003.

Rinberg, D., Koulakov, A., Ollinger, F., Gelperin, A., 2004. Mitral cell responses in awake and anesthetized mice. Program No. 139.11 2004 Abstract Viewer/Itinerary planner. Wash. DC, Soc. Neurosci. (Online).

Rinberg, D., Koulakov, A., Gelperin, A., 2006. Sparse odor coding in awake behaving mice. J. Neurosci. 26 (34), 8857–8865. https://doi.org/10.1523/JNEUROSCI.0884-06.2006. PMID: 16928875; PMCID: PMC6674368.

Shmuel, R., Secundo, L., Haddad, R., 2019. Strong, weak and neuron type dependent lateral inhibition in the olfactory bulb. Sci. Rep. 9 (1), 1602. https://doi.org/10.1038/s41598-018-38151-9.

Shusterman, R., Smear, M.C., Koulakov, A.A., Rinberg, D., 2011. Precise olfactory responses tile the sniff cycle. Nat. Neurosci. 14 (8), 1039–1044. https://doi.org/10.1038/nn.2877.

Tan, J., Savigner, A., Ma, M., Luo, M., 2010. Odor information processing by the olfactory bulb analyzed in gene-targeted mice. Neuron 65 (6), 912–926. https://doi.org/10.1016/j.neuron.2010.02.011.

Uchida, N., Poo, C., Haddad, R., 2014. Coding and transformations in the olfactory system. Annu Rev. Neurosci. 37, 363–385. https://doi.org/10.1146/annurev-neuro-071013-013941.

Vaaga, C.E., Westbrook, G.L., 2016. Parallel processing of afferent olfactory sensory information. J. Physiol. 594 (22), 6715–6732.

Wachowiak, M., 2011. All in a sniff: olfaction as a model for active sensing. Neuron 71 (6), 962–973. https://doi.org/10.1016/j.neuron.2011.08.030.

Welch, P., 1967. The use of fast Fourier transform for the estimation of power spectra: A method based on time averaging over short, modified periodograms. IEEE Trans. Audio Electro 15 (2), 70–73. https://doi.org/10.1109/tau.1967.1161901.

Wood, F., Black, M.J., 2008. A nonparametric Bayesian alternative to spike sorting. J. Neurosci. Methods 173 (1), 1–12.

Yokoi, M., Mori, K., Nakanishi, S., 1995. Refinement of odor molecule tuning by dendrodendritic synaptic inhibition in the olfactory bulb. Proc. Natl. Acad. Sci. USA 92 (8), 3371–3375. https://doi.org/10.1073/pnas.92.8.3371. PMID: 7724568; PMCID: PMC42168.

Yoon, Y.G., Kim, T.H., Jeong, D.W., Park, S.H., 2011. Monitoring the depth of anesthesia from rat EEG using modified Shannon entropy analysis. Annu Int Conf. IEEE Eng. Med Biol. Soc. 2011, 4386–4389. https://doi.org/10.1109/IEMBS.2011.6091088.